MCB Accepts, published online ahead of print on 1 June 2010
Mol. Cell. Biol. doi:10.1128/MCB.00949-09

The p38 MAPK promotes cell survival in response to DNA damage but is not required for G_2 DNA damage checkpoint in human cancer cells

Mark S. Phong[1,5], Robert D. Van Horn[2], Shuyu Li[3], Gregory Tucker-Kellogg[1,6], Uttam Surana[4,5], *Xiang S. Ye[2]

[1]Lilly Singapore Center for Drug Discovery, Pte Ltd, (Eli Lilly & Company), Singapore

[2]Cancer Research Division, Lilly Research Labs, Lilly Corporate Center, Eli Lilly & Company, Indianapolis, IN 46285, USA

[3]Translational Science, Lilly Research Labs, Lilly Corporate Center, Eli Lilly & Company, Indianapolis, IN 46285, USA

[4]Institute of Molecular and Cell Biology, Agency of Science, Technology and Research, Singapore

[5]Department of Pharmacology, Yong Loo Lin School of Medicine, National University of Singapore, Singapore

[6]Department of Biological Sciences, Faculty of Science, National University of Singapore, Singapore

*For Correspondence:

Xiang S. Ye, PhD

Lilly Research Labs

Lilly Corporate Center, DC 0546

Indianapolis, IN 46285

Phone: 317-277-1467, Fax: 317-276-6510, email: ye_xiang_s@lilly.com

Running Title: p38 promotes cell survival after DNA damage

Word Count: Materials and methods: 862, Introduction, Results & Discussion: 4714

Abstract

The p38 MAPK is rapidly activated by stresses and is believed to play an important role in stress response. While Chk1 is known to mediate the G_2 DNA damage checkpoint control, p38 is also reported to have an essential function in this checkpoint control. Here, we have investigated further the roles of p38 and Chk1 in G_2 DNA damage checkpoint in cancer cells. We find that although p38 activation is strongly induced by DNA damage, its activity is not required for the G_2 DNA damage checkpoint. By contrast, Chk1 kinase is responsible for the execution of G_2 DNA damage checkpoint control in p53-deficient cells. Inhibition of p38 activity has no effect on Chk1 activation and γH2AX expression. Global gene expression profiling of cancer cells in response to TNFα revealed that p38 plays a strong pro-survival role through coordinated down-regulation of pro-apoptotic genes and up-regulation of pro-survival genes. We show that inhibition of p38 activity during G_2 DNA damage checkpoint arrest triggers apoptosis in a p53-independent manner with a concurrent decrease in the level of Bcl2 family proteins. Our results suggest that although p38 MAPK is not required for the G_2 DNA damage checkpoint function, it plays an important pro-survival role during G_2 DNA damage checkpoint response through up-regulation of the Bcl2 family proteins.

Introduction

The p38 MAPK was originally identified as a 38 kD protein that undergoes rapid tyrosine phosphorylation in response to stress (17). Significant progress has been made in the past decade to understand the p38 signal transduction pathway and the biological processes regulated by p38 MAPK. The p38 MAPK is activated in response to stress related stimuli such as UV light(28), heat (40), osmotic shock (34,40), endotoxins (18) and inflammatory cytokines like TNF-α and IL-1 (27,35). The p38 pathway is implicated in inflammatory response as p38 activation induces pro-inflammatory cytokines and enzymes such as Cox-2 which controls connective tissue remodeling, and inflammation related adhesion proteins such as VCAM-1 (37), thus making p38 MAPK signaling an attractive therapeutic target for the mitigation of inflammatory diseases (42). This has led to the creation of biochemical inhibitors targeting p38 kinase (7,20). The latest generation of these inhibitors is highly potent and selective; raising possibilities that therapy involving p38 inhibitors may one day be an effective treatment for inflammatory diseases.

Recently p38 MAPK activity has been reported to be critical for the G_2 DNA damage checkpoint control in response to DNA damage by UV irradiation (5,6,32) or by genotoxic agents (19,26). The primary mechanism of p38 involvement in G_2 DNA damage checkpoint is thought to be mediated through inhibition of CDC25B/C phosphatases which are required for the activation of CDK1 to initiate mitosis (5,32). Structural analysis of the p38 binding site, however, suggests that it is unlikely that p38 could interact directly with CDC25B. Instead, its direct downstream target MAPKAPK2

(MK2) is implicated as the mediator of p38-dependent G_2 DNA damage checkpoint control (32).

The ability of cancer cells to establish cell cycle arrest in response to genotoxic agents is one of the reasons for resistance to chemotherapy (8). Cancer cells that undergo a reversible cell cycle arrest in response to genotoxic agents such as adriamycin (Doxorubicin HCL) and cisplatin have the ability to survive chemotherapy and continue proliferation post therapy, leading to poor patient outcomes. The implication that p38 activity is necessary for G_2 DNA damage checkpoint arrest provides an exciting possibility for p38 inhibitor as chemo-sensitizer to enhance efficacy of chemotherapies by abrogating the G_2 DNA damage checkpoint to promote cancer cells to enter mitosis prematurely.

Both p38 and Chk1 are activated by DNA damage in mammalian cells and both are believed to directly inactivate CDC25 family of protein phosphatases to prevent mitotic entry in the presence of DNA damage (25,45,46). Paradoxically, inhibition of either p38 or Chk1 has been shown to be sufficient to abrogate the G_2 DNA damage checkpoint (5,21,45). The role of the p38 MAPK pathway in the G_2 DNA damage checkpoint of cancer cells has recently been called into question by the observation that transformed cells do not delay entry into mitosis upon activation of the p38 stress pathway by anisomycin (33). Furthermore, it has been shown recently that RNAi-mediated inhibition of Chk1, but not Chk2 or MK2, in HeLa and H1299 cancer cells abrogates DNA-damage induced S-phase or G_2-phase arrest (46). The requirement for p38 in the G_2 DNA damage checkpoint control may be cell type specific, or may depend on the type of DNA damage. While p38 is activated by both ionizing and UV radiation, the p38/MK2 pathway is

reported to be only essential in G_2 DNA damage checkpoint in the absence of p53 (39). It should be noted that older generation of small molecule inhibitors of p38 kinase was used at very high concentrations in many earlier studies, raising the possibility of off-target effects (1,10). In this study, we revisited the role of p38 activity in the G_2 DNA damage checkpoint control in response to several types of DNA damage, and investigated the relationship between Chk1 and p38 kinases in G_2 DNA damage checkpoint control in tumor cells with or without functional p53. We also used newer generation of small molecule kinase inhibitors which are more potent and selective at physiologically relevant concentrations and independently confirmed and corroborated the small molecule kinase inhibitor activity with siRNA-mediated inhibition.

We demonstrate that while p38 is rapidly and strongly induced by DNA damage, inhibition of p38 activity with a potent and selective inhibitor LY479754 or siRNA knock-down does not compromise the ability of cancer cells to mount an effective, checkpoint-mediated G_2 arrest in response to adriamycin, MMS or UV-induced DNA damage. In contrast, the chemical inhibition and siRNA knock-down of Chk1 efficiently abolishes the G_2 DNA damage checkpoint in cancer cells with deficient p53. Using an unbiased whole genome transcriptional analysis, we identified a strong link between p38 activation and the suppression of anti-apoptotic signaling in TNF-α-treated cells. Extending these findings to the G_2 DNA damage checkpoint context, we show that inhibition of p38 results in a dramatic increase in apoptosis of cells arrested in G_2 in response to DNA damage. Based on our observations, we propose that although not required for the G_2 DNA damage checkpoint control, p38 plays an important cytoprotective role through the regulation of apoptotic and survival pathways to allow cells to recover from DNA damage.

Results

p38 MAPK is activated by DNA damage at different stages of the cell cycle

The p38 MAPK is known to be activated in response to DNA damage. We first assessed if p38 activation is associated with G_2 arrest induced by different modes of DNA damage. For these experiments, we used different sources of DNA damage that induce a G_2 arrest in p53-deficient HeLa cells (Fig. 1A). In conjunction with the establishment of G_2 cell cycle arrest, p38 is strongly activated by increasing doses of UV-B irradiation (Fig. 1B), 0.01% MMS (Fig. 1C) and 160nM adriamycin (data not shown, also see Fig. 1D) with similar kinetics. To further confirm that activation of p38 is closely correlated with G_2 arrest, we synchronized HeLa cells at G_1/S using the double thymidine block/release protocol before imposing DNA damage by addition of adriamycin and followed the cell cycle progression by monitoring multiple parameters. Indeed, adriamycin treatment caused G_2 arrest and a sustained activation of p38 (Fig. 1D).

To investigate if p38 activation occurs specifically during G_2 DNA damage checkpoint-mediated arrest, HeLa cells were synchronized in G_1 by serum-starvation (Fig. 1E), in early S phase by double thymidine block (Fig. 1F) or in G_2 by CDK1 inhibitor (RO-3306) (Fig. 1G) and then released into fresh growth medium containing 0.01% MMS. Cells were subsequently monitored for the activation status of Chk1, p38, and MAPKAPK-2 (MK2) using the respective phosphorylation-specific antibodies. As shown in Fig. 1E-G, p38 and Chk1 are rapidly activated after MMS treatment in HeLa cells synchronized at different stages of the cell cycle. Activation of p38 occurred earlier than that of Chk1 in

G_1 and S-phase cells, whereas p38 and Chk1 activation in G_2-phase cells followed a similar kinetics (Fig. 1E-G).

Inhibition of p38 does not abrogate G_2 DNA damage checkpoint control

To test whether p38 pathway activity is essential for the G_2 DNA damage checkpoint in response to DNA damage, we investigated the effect of chemical inhibition of the p38 pathway activity with LY479754 (p38i), a highly potent and selective p38 inhibitor (7,11), on G_2 DNA damage checkpoint-mediated arrest in both unsynchronized (Fig. 2A) and synchronized (Fig. 2B) HeLa cells treated with adriamycin. Nocodazole, a microtubule depolymerizing agent, was added to the medium to trap in mitosis cells that escape the checkpoint arrest in unsynchronized cells. Despite a strong inhibition of p38 activity, seen as complete inhibition of p38-mediated phosphorylation of MK2, HeLa cells were still able to mount an effective G_2 DNA damage checkpoint control in response to adriamycin treatment. Inhibition of p38 did not lead to any significant increase in the mitotic marker phospho-histone H3 over a 24 hour period. Similarly, another small molecule kinase inhibitor, SB203580, at concentrations above that needed for completion inhibition of p38, also had no effect on the G2 DNA damage checkpoint, as HeLa cells remained arrested in G2 during a synchronized G2/M progression (data not shown). Inhibition of MK2 also showed no effect on checkpoint activity (Fig. 2B). In contrast, inhibition of Chk1 with a selective Chk1 inhibitor (Fig. 2A&B) or ATM/ATR inhibition with caffeine (Fig. 2B) in an identical experimental setting led to a dramatic increase in phospho-histone H3 levels, indicating effective abrogation of G_2 DNA damage checkpoint. Consistent with checkpoint abrogation, inhibition of Chk1 or ATM/ATR led to a marked decrease in Cdk1 phosphorylation on Tyr15 (Fig. 2B). On the other hand, inhibition of p38 had no effect on the level of Cdk1 phosphorylation at Tyr15 which

remained high (Fig. 2B). Furthermore, abrogation of the G_2 DNA damage checkpoint with either a Chk1 inhibitor or caffeine occurred in the presence of high p38 and MK2 activities (Fig. 2B).

These analyses were followed by confocal immunofluorescence microscopy in HeLa cells. Cells treated with either adriamycin alone or adriamycin+p38i for 21 hours had high levels of γH2AX in the nucleus. These cells were arrested at G_2 as indicated by cytoplasmic accumulation of cyclinB1 and 4N DNA content (data not shown; also see Fig. 1A). No mitosis was observed in the p38-inhibitor treated cells under the microscope. In contrast, HeLa cells that were treated with adriamycin+Chk1 inhibitor underwent mitosis as evidenced by mitotic spindles, condensed DNA and strong phospho-histone H3 signal, indicating effective abrogation of G_2 DNA damage checkpoint (data not shown). Western blot analysis further showed that inhibition of p38 MAPK has no apparent impact on γH2AX expression and activation of Chk1 (Fig. 2C). This shows that despite potent inhibition of p38 MAPK pathway, DNA damage response to adriamycin and MMS is unimpeded leading to a strong G_2 DNA damage checkpoint-mediated cell cycle arrest.

Previous reports first implicating p38 as a critical kinase in G_2 DNA damage checkpoint function utilized UV irradiation as a source of DNA damage (5). Since p38 activity does not appear to be necessary for adriamycin or MMS induced G_2 DNA damage checkpoint arrest, we thus wanted to investigate further a role of p38 activity in response to UV-induced DNA damage. Both synchronous and asynchronous HeLa cell cultures were exposed to UV radiation and incubated with either p38 or Chk1 inhibitors immediately after UV treatment. Nocodazole was added to the cultures to trap in mitosis cells that had

escaped from G_2 DNA damage checkpoint-mediated arrest. Cells were harvested for analysis of various mitotic markers after 24 h. Again, while pharmacological inhibition of p38 and MK2 did not lead to any significant increase in mitotic index over 24 h, inhibition of Chk1 led to a dramatic increase in mitotic index and phospho-histone H3 over the same time period (Fig. 2D&E). These results suggest that as in the case of adriamycin treatment, UV damage-induced G_2 arrest is not dependent on p38 activity.

To rule out the possibility of off-target effects by chemical inhibitors used in the experiments, we performed a series of siRNA knock-down experiments targeting p38α, MK2 and Chk1 in HeLa cells with 2 specific siRNA oligos for each gene. Both siRNA oligos effectively inhibited their target gene expression as determined by Western blot analysis (Fig. 3A). Cells were transfected with appropriate siRNA, transferred to fresh growth medium after 48 hrs and were then treated with adriamycin for additional 24 h. Consistent with the data obtained using the small molecule kinase inhibitors, knock-down of Chk1 using siRNA also abrogated the G_2 DNA damage checkpoint in the presence of high p38 activity, as evidenced by a decrease in the CDK1 Tyr15 phosphorylation and an increase in the histone H3 phosphorylation and mitotic index (Fig. 3A&B). Similarly, siRNA-mediated inhibition of Chk1 also abrogated UV induced G_2 DNA damage checkpoint arrest (Fig. 3B). In contrast, knock-down of p38α or MK2 did not affect the G_2 DNA damage checkpoint arrest induced by adriamycin or UV treatment (Fig. 3A&B).

Lastly, to show that the lack of any effect by p38 inhibition on the G_2 DNA damage checkpoint-induced arrest was not a phenomenon specific to HeLa cells, we conducted similar experiments using A549 (lung Cancer), U2OS (osteosarcoma) and Calu-6 (lung) cell-lines. Similar to the results obtained with HeLa cell, inhibition of p38 also had no

impact on the ability of these cancer cell lines to mount a strong G_2 DNA damage checkpoint-imposed cell cycle arrest in response to adriamycin treatment (Fig. 3C). Again, inhibition of Chk1 was able to abrogate the adriamycin induced G_2 arrest in the p53 deficient Calu-6 cells, but not in p53-proficient A549 and U2OS cells as reported previously (22,29). In addition, we attempted to reproduce the effect of UV-C irradiation in U2OS cells exactly as previously reported (32). We found that two independent siRNA oligonucleotide targeting MK2, of which one was the same siRNA oligos previously published (36), effectively inhibited MK2 expression (Fig. 3D). Contrary to the previous report (36), however, inhibition of MK2 by RNAi had no effect on histone-H3 phosphorylation in response to $20J/M^2$ UV-C irradiation as monitored by Western blotting or flow cytometry after 18 hours in a nocodazole mitotic trap assay (Fig. 3D&E). Consistent with our siRNA results for HeLa cells, these results indicate that MK2 inhibition does not abrogate the G_2 DNA damage checkpoint function. In addition, RNAi-mediated inhibition of MK2 also had no effect on γH2AX expression and activation of p38 MAPK in response to UV-C treatment (Fig. 3D). We also noticed that a significant fraction of U2OS cells lost viability when exposed to $20J/M^2$ UV-C. Taken together, these results demonstrate that although the p38 pathway is induced robustly in response to DNA damages, its activity is not required for the execution or maintenance of G_2 DNA damage checkpoint control.

Non-genotoxic activation of p38 does not inhibit mitotic entry

If p38 activity is indeed important for execution of G_2 DNA damage checkpoint, then DNA-damage independent activation of p38 would be expected to impede progression into mitosis by untimely engagement of the G_2 DNA damage checkpoint. Therefore, we investigated the effect of non-genotoxic activation of p38 by anisomycin, a potent

antimicrobial agent, on the onset of mitosis. Short term exposure to anisomycin at 2μg/ml is not known to cause DNA damage, but strongly induces the p38 signaling pathway at our hands (11). HeLa cells were first synchronized at the G_2 boundary with a CDK1 inhibitor (43) and then released in the presence or absence of anisomycin. Cell cycle progression from G_2 was then followed up to 6 h after release from CDK1 inhibitor block. As expected, p38 activation was strongly induced by anisomycin but high p38 activity had no impact on the ability of synchronized Hela cells to enter mitosis rapidly (Fig. 4).

p38 MAPK plays a pivotal role in immediate early stress response and cell survival

To uncover a new role for p38 activity in DNA damage response outside the context of G_2 DNA damage checkpoint, we returned to the original context of p38 activation in stress response. We first demonstrated that the p38i effectively inhibited TNFα induced activation of p38 signaling (data not shown).We then profiled effects of p38 inhibition on global gene expression in cancer cells induced by TNF-α. Calu-6 lung cancer cells were treated with TNF-α and p38 inhibitor (LY479754) across a time-course. Samples were run on Affymetrix HG-U133plus2 gene chips to enable an unbiased assessment of transcriptional changes in response to TNF-α and p38 inhibition across time.

A total of 853 transcripts showed significant expression changes between TNF-α treated cells and DMSO controls in at least one of the 5 time points analyzed (data not shown). To understand the primary effects of TNF-α on gene expression, we focused on transcription changes at 1 h time point after TNFα treatment and identified a total of 115 transcripts corresponding to 72 unique genes which were differentially expressed. Based

on their expression patterns across the 5 time points revealed by hierarchical clustering, they fall into 4 distinct groups (Fig. 5A). The first group includes 10 genes; among them 9 are immediate early response genes encoding transcription factors (Supplementary Table 1). Not surprisingly, this group of genes responded most rapidly and transiently to TNF-α treatment (Fig. 5A). The second group is the largest, with 31 genes consisting of cytokine, chemokine, growth factor genes and genes implicated in stress response (Supplementary Table 1). This group also responded to TNF-α rapidly, peaking from 1 to 2 hours and then declined more slowly than the genes in the first group (Fig. 5A). The third group includes 22 genes that responded to TNF-α more slowly and in a lower magnitude than the first 2 groups (Fig. 5A). Most of the genes in this group have functions related to immune regulation (Supplementary Table 1). The fourth group of 9 genes negatively responded to TNF-α treatment (Fig. 5A and supplementary Table 1). Taken together, these genes which were differentially regulated by TNF-α are mostly associated with stress and immune responses, consistent with the expected function of TNF-α signaling.

Treatment of Calu-6 cells with a selective p38 kinase inhibitor (p38i), LY479754, alone caused expression changes only in three genes across time compared to the DMSO controls, further demonstrating the extraordinary selectivity of this kinase inhibitor (data not shown). One of the genes that was down regulated is COX2, a known p38 target gene (15), while FADD, a pro-apoptotic component of the FAS receptor pathway, was up-regulated in the early time points (Fig. 5B). Among the 853 transcripts regulated by TNFα, the p38 kinase inhibitor completely blocked the expression changes of 260 transcripts and also significantly inhibited changes in the expression levels of another 185

transcripts induced by TNFα (Supplementary Table 2). Together, 445 (52%) of TNFα regulated genes responded to inactivation of p38, providing strong evidence for a significant role of p38 MAPK in TNFα-induced stress response. Furthermore, inactivation of p38 abolished > 70% of the expression changes induced by TNFα at the 1 h time point. As shown in Fig. 5A, expression changes in cluster 1 and 2 genes that responded most rapidly to TNFα were also most strongly inhibited by the p38i, whereas, genes in cluster 3 that responded more slowly and in a lower magnitude to TNFα were much less affected by p38 inactivation. The data further demonstrate that p38 MAPK plays a pivotal role in early cellular responses to TNFα.

Among many genes, networks and canonical pathways that were affected by p38 inhibition of TNF-α treatment, we found a significant representation of genes modulating the anti-apoptosis and cell survival pathway (Fig. 5A; supplementary Table S2). In response to TNF-α, Calu6 cells immediately activated a potent cell survival response including up-regulation of pro-survival pathways such as BCL-xl, IL6, Myc and EGR (13,41,44), and also down-regulation of pro-apoptotic signaling components such as TRADD and FADD (Fig. 5B). Inhibition of p38 significantly reversed these pro-survival responses, resulting in a recovery of TRADD and FADD and a significant decrease in BCL-xl, IL6, EGR and Myc (Fig. 5B).

Gene expression changes were confirmed at the protein level by Western blotting. Inhibition of p38 pathway with LY479754 indeed led to a significant decrease in the levels of BCL2 and BCL-xl and the reversal of decreased FADD expression in the TNFα-treated cells, in line with results from the gene expression study (Fig. 5C).

Concurrently, inhibition of p38 also led to an early induction of PARP cleavage, a cellular marker for apoptotic cell death. To further confirm and quantify apoptotic cell death, we determined the apoptosis index (% of cells expressing cleaved-PARP) of TNFα-treated cells in the presence of p38i. We found that p38i in combination with TNFα indeed led to increased apoptosis compared to TNFα alone as early as 3 hours after treatment (Fig. 5D). Together, these results strongly suggest that p38 signaling plays an important role in immediate early response and in induction of pro-survival/anti-apoptotic signaling in response to TNF-α stress.

Inhibition of p38 in response to DNA damage leads to cell death via inhibition of BCL2 family proteins

The discovery that p38 inhibition results in a strong dampening of anti-apoptotic gene expression in response to TNF-α led us to reason that p38 activity may play a role in modulating apoptotic induction in the context of DNA damage. If so, then inhibition of p38 should result in induction of apoptosis of cells treated with DNA damaging agents. To test this hypothesis, both synchronous and asynchronous HeLa (p53-deficient) and A549 (p53-proficient) cells were treated with adriamycin or MMS in the presence of the p38i, LY479754, for up to 48 h and assayed for the apoptotic markers, namely, cleavage of caspase 3 or 7 and PARP. A dose escalation experiment with the p38 inhibitor in combination with adriamycin showed a corresponding increase in cleaved-caspase-3 levels measured as apoptotic index at 48 hours post treatment (Fig. 6A). Consistent with this, additional experiments with siRNA targeting p38α and MK2 in HeLa cells also showed a marked increase in apoptotic markers in combination with adriamycin but not in cells treated with adriamycin alone or non-specific siRNA in the presence of

adriamycin (Fig. 6B). Inhibition of p38 with LY479754 also led to a dramatic increase in PARP cleavage in p53-positive A549 cells after DNA damage by adriamycin (Fig. 6C)

Since we observed a strong inhibition of BCL2 family gene expression upon p38 inhibition in TNF-α treated cells, we wanted to test if inhibition of BCL2 family proteins may provide a mechanistic explanation for a role of p38 in regulation of apoptosis following DNA damage. We find that p38 inhibition in response to both adriamycin (Fig. 6C) and MMS (Fig. 6D) damage leads to a dramatic decrease in BCL-xl protein levels, matched with a concordant increase in the level of PARP cleavage. Finally, using multi-parametric cytometry, we also find that the inhibition of p38 induced apoptosis of cells that were largely arrested in the G_2 phase in the presence of DNA damage (Fig. 6E). Taken together, these observations suggest that p38 activity is an integral part of the pro-survival signaling network induced in response to DNA damage.

Discussion

In this study, we show that p38 activation is strongly induced by DNA damage and is correlated with G_2 arrest. Contrary to prior reports (5,26,32). However, our data strongly suggest that p38 pathway activity is not necessary for the G_2 DNA damage checkpoint function. Furthermore, inhibition of Chk1 or ATM/ATR kinase abrogates the G_2 DNA damage checkpoint in the presence of high p38 activity. While HeLa cells were the primary cell model used in this study, we also show that the inhibition of p38 activity was unable to abrogate G_2 DNA damage checkpoint control in Calu-6, A549 and U2OS cell-lines. In concordance with previous reports (24,29), we find that pharmacological inhibition of Chk1 alone with a selective small molecule kinase inhibitor or siRNA knock-down was not sufficient to abrogate the G_2 DNA damage checkpoint in the p53 proficient cells. Corroboration of pharmacological inhibition using small molecule kinase inhibitors with siRNA knock-down rules out the possibility that the observations may be caused by off-target activity of the chemical kinase inhibitors. Conversely, non-genotoxic activation of p38 by anisomycin in G_2 was not sufficient to activate the G_2 DNA damage checkpoint. Taken together, our results strongly suggest that neither the suppression of p38 activity nor its non-genotoxic activation has an impact on G_2 DNA damage checkpoint activity.

Inhibition of CDC25B/C phosphatase activity is believed to be the primary mechanism through which the p38 pathway participates in the G_2 DNA damage checkpoint control (5,32). This prevents the formation of active CDK1/cyclinB complex, thus blocking progression into mitosis. We find that effective inhibition of p38 activity had no discernable impact on the level of CDK1 Tyr15 phosphorylation in response to

adriamycin treatment. This lack of effect of p38 inhibition on CDK1 activation through Tyr15 dephosphorylation by CDC25 provides further biochemical evidence in support of the proposition that p38 does not play an important role in G_2 DNA damage checkpoint control. Alternatively, as Chk1 kinase is activated in a very similar manner in response to DNA damage, potential pathway redundancies may mitigate the effect of p38 inhibition on CDC25B activity. In p53 deficient cells, however, we find that inactivation of Chk1 alone effectively abrogated G_2 DNA damage checkpoint. Furthermore, the abrogation of G_2 DNA damage checkpoint by Chk1 inactivation occurs in the presence of high p38 kinase pathway activities. Therefore, in agreement with many previous publications (4,9) our data suggest that the Chk1 signaling pathway is primarily responsible for the inactivation of CDK1 in response to DNA damage to prevent cells' progression into mitosis.

As we were interested in the exciting possibility of using potent and selective p38 kinase inhibitors as chemo-sensitizers to enhance anticancer efficacy of chemotherapies, the inability of a highly selective and potent p38 kinase inhibitor to abrogate G_2 DNA damage checkpoint comes as a surprise. A closer examination of earlier publications, however, reveals a certain degree of discrepancies concerning the role of p38 in G_2 DNA damage checkpoint control in response to different types of DNA damage and the function of p53 (5,32,39). In addition, earlier studies used older generation of p38 kinase inhibitors at very high concentrations (5,39). At such high concentrations, it is likely that these p38 kinase inhibitors may have off-target activities as shown recently (1,10). Our data are consistent with a more recent report that demonstrates that using the RNAi approach, only Chk1 but not Chk2 or MK2 is responsible for G_2 DNA damage checkpoint control in cancer cells (46). Furthermore, it is also recently shown that the p38

pathway response at the G_2 DNA damage checkpoint is strongly attenuated in transformed cells (33). Earlier studies that implicated p38 activity in G_2 DNA damage checkpoint control were performed in untransformed human cells and mouse embryonic fibroblasts (5,36,39). However, untransformed mammalian cells have intact p53 and Chk1 functions. Thus, it is unconceivable that normal, untransformed mammalian cells with functional p53 and Chk1 would depend on p38 alone for G_2 DNA damage checkpoint function but not cancer cells which are frequently deficient in p53 function. Indeed, similar to the findings in p53 proficient cancer cells, we find that inhibition of p38 activity by the small molecule inhibitor LY479754 was unable to abrogate the G_2 DNA damage checkpoint in HUVEC cells in response to adriamycin treatment (data not shown). Together, our results, therefore, rule out the feasibility of developing a p38 inhibitor as a chemo-sensitizer to enhance efficacy of chemotherapies.

To identify a new role for p38 activity in DNA damage response outside cell cycle checkpoint control, we conducted a genome-wide gene expression profiling analysis of the effect of p38 inhibition in response to TNF-α stress. We find that inhibition of p38 dramatically dampens the immediate early transcriptional response and the ability of cancer cells to mount an effective anti-apoptotic/pro-survival response to TNF-α. Moreover, the pro-survival signaling induced immediately after exposure to TNF-α consisted of the down-regulation of pro-apoptotic factors such as FADD and TRADD and the up-regulation of anti-apoptosis components including anti-apoptosis BCL2 family proteins.

Testing the hypothesis derived from the analysis of transcriptional data in the context of DNA damage, we find that inhibition of p38 in combination with adriamycin leads to

strong induction of apoptosis. Increased apoptosis was observed in both p53 deficient HeLa cells as well as in p53 proficient A549 cells, implying that the link between p38 activity and pro-survival signaling does not depend on p53 status. Further mechanistic studies in the context of DNA damage show that p38 may confer its pro-survival effect in response to DNA damage through the regulation of anti-apoptotic BCL2 family proteins. Consistent with this notion, we find that chemical inhibition or siRNA knock-down of p38 in the presence of adriamycin or MMS treatment leads to a dramatic decrease in BCL2 and BCL-xl. The data suggests that p38 activity, while not connected directly with the proper functioning of the G_2 DNA damage checkpoint, plays a pivotal role in response to DNA damage.

We note that the link between p38 activity, pro-survival signaling in response to DNA damage and stress may be unexpected, given the strong association of p38 activation with FasL and TNF-α induced apoptosis (14). The behavior of DNA damaged cells in which checkpoint has been abrogated may be of some relevance. We have observed that Chk1 inhibitor or caffeine mediated abrogation of G_2 DNA damage checkpoint occurs with high p38 activity. This implies that while inhibition of p38 in conjunction with DNA damage leads to increased apoptosis, high p38 activity alone does not prevent apoptosis. Thus, in the case of Chk1 inhibition-mediated mitotic catastrophe, other apoptosis inducing factors may override the cytoprotective effects of p38 activity. Although the underlying mechanistic rationale for this observation is unclear, these observations suggest that there may be a more complex, and context-specific relationship between p38 and apoptosis induction. From a teleological perspective, it can be argued that in an early response to stress, p38 signaling promotes cell survival to facilitate the evaluation of the extent of damage to the cell. Once the G_2 DNA damage checkpoint is breached, p38

mediated pro-survival signaling is no longer required or sufficient, as elimination of cells undergoing mitotic catastrophe would be in the best interest of multicellular organisms.

Our assertion that p38 plays a role in cell survival is supported by a number of recent reports linking this signaling pathway to increased levels of BCL2 and BCL-xl in response to DNA damage and stress (12,23). Furthermore, chemical inhibition of p38 has been strongly associated with increased chemosensitivity in cancer cells (16,31). Based on our study and correlative evidence from other reports, we propose a new role for p38 in the context of response to DNA damage (Figure 7). According to this scheme, while p38 is activated in response to DNA damage resulting in a G_2 DNA damage checkpoint-mediated cell cycle arrest, its activity is not required for the activation or maintenance of the G_2 DNA damage checkpoint. Instead p38 activity in response to DNA damage induces pro-survival signaling to prevent the onset of pre-mature apoptosis in the immediate aftermath of stress of DNA damage and allows recovery from DNA damage. This anti-apoptosis response likely allows cells to ascertain the extent of damage and to response accordingly. It appears that the role of p38 in the regulation of apoptosis is context dependent and may switch from pro-survival to pro-apoptosis depending on both the timing and physiological context of the stress induction. Clearly, elucidation of the full mechanism of p38 in the regulation of apoptosis would require further investigations.

Methods and Materials

Cell Culture and Synchronization

All cancer cell lines were obtained from ATCC. HeLa cells were grown in DMEM media supplemented with 10% FBS, Calu-6 cells were grown in MEM media supplemented with 10% FBS, 1% sodium pyruvate and 1% HEPES, A549 cells were grown in RPMI1640 media, supplemented with 10% FBS and U2OS cells were grown in McCoy 5A media supplemented with 10% FBS. All cell culture media and additives were purchased from GIBCO (Invitrogen, Carlsbad CA, USA). All cells were grown in a cell culture incubator at 37^{o}C and 5% CO_2 in T75 or T150 tissue culture flasks (Corning, Lowel, MA, USA). Cells were synchronized at G1 using double thymidine block/release or at G2 using a selective CDK1 inhibitor as previously described (11).

Antibodies, Western blot Analysis and Immuno-fluorescence Microscopy

Rabbit polyclonal antibody to phospho-histone H3, Ser10 (Cat No. 06-570) was purchased from Upstate Inc. (Charlottesville, VA). Rabbit polyclonal anti-phospho-p38 (Cat No. 9216), anti-phospho-MAPKAPK2 (MK2) (Thr334) (Cat No. 3041), anti-phospho-Chk1 (Ser 345) (Cat No. 2341), anti-phosph-HSP27(ser 17) (Cat No. 2404), anti-cl-Casp3 (Cat No.9661), anti-cl-Casp7, D198 (Cat No. 9491), anti-α/β Tubulin (Cat No.2148), anti-BCL2 (Cat No. 2872), anti-BCL-xl (Cat No. 2762), anti-γ-H2AX (Cat No. 9718), anti-FADD (Cat No. 2782), anti-p38α (Cat No. 9218), anti-β actin (Cat No. 4967), and mouse monoclonal anti-c-PARP, D214 (Cat No. 9546), were all purchased from Cell-Signaling Technologies Inc (Beverly, MA, USA). Anti-CyclinB1 (Cat No. 610220) was purchased from BD Transduction Laboratories (San Jose, CA, USA). HRP conjugated secondary antibodies were purchased from Amersham (Piscataway, NJ, USA)

and Alexa-Fluor linked secondary antibodies were purchased from Invitrogen (Carlsbad, CA, USA).

Protein lysates of cultured cells were prepared in a lysate buffer containing a cocktail of phosphatase and protease inhibitors and Western blotting was performed as previously described (11). Luminescent substrate detection was performed using the ECL Advance or ECL plus chemi-luminescent kit (Amersham, Piscataway NJ, USA). Chemi-luminescent signal was detected using a high resolution GE Gel-blot imager.

Cells were plated for confocal microscopy in Lab-Tek 4 Chamber slides (Fisher Scientific). Cells were fixed with 4% para-formaldehyde in PBS and then permeabilized with 0.2% Triton-X 100. After blocking for 1 hour in 1% BSA in PBS, the cells were incubated with anti-γ-H2AX (1:200), and anti-cyclin B1 (1:500) antibodies in block solution for one hour at room temperature. The cells were washed 3X in PBS and incubated with secondary antibody (1:1000) and DNA stain (Sytox Green, Invitrogen, 1:20000) for one hour at room temperature. The cells were washed 3X with PBS and imaged. Cell imaging was acquired with a Zeiss LSM510 confocal microscope.

Use of Chemical Agents and Inhibitors

The use of biochemical inhibitors and chemical genotoxic compounds in this study was performed as previously described (11,47). Chemical inhibitors used in this study were synthesized by Lilly chemists. Kinase inhibitors used in this study were: p38α/β inhibitor LY479754 (7,11), MAPKAPK2 (MK2) inhibitor(38) and Chk1 inhibitor PF-00477736 (2). CDK1 inhibitor RO-3306 was purchased from Calbiochem (San Diego, CA, USA).

All other chemical reagents used in this study were purchased from Sigma Aldrich (St Louis, MI, USA).

siRNA Transfection

Transfection of 21-nucleotide siRNA duplexes (Qiagen Sciences, Germantown MD,USA) for targeting endogenous genes was carried out using Lipofectamine RNAimax (Invitrogen, Carlsbad CA, USA) as previously described in low serum (Opti-mem) medium (11). The following validated commercial siRNAs from Qiagen were used in this study: si-p38α: (SI00300769, SI00605157), si-MK2: (SI02223697, SI00288246), si-Chk1: (SI0266000, SI00299859). In addition, a MK2-specific siRNA oligonucleotide described by Manke et al. (36) was synthesized by Dharmacon and used.

Acumen Explorer High Content Imaging Analysis

HeLa cells were plated in 96 well Beckman Dickinson Biocoat plates at 2000 cells per well in 100 µl medium, and incubated in 5% CO2 at 37^{o}C for 24 hours before treatment with compounds diluted in growth media with 10% FBS and 0.25% DMSO. All liquids were handled with an automated 96-channel pipette (Multimek 96, BECKMAN) to process the plates. Cells were fixed with the Prefer fixative (Anatech LTD, MI, USA) at 25^{o}C for 30 min, permeabilized with 0.1% Triton X100 in PBS (GIBCO, Carlsbad, CA) for 15 min, and then treated with RNase A (50µg/ml in PBS) (Sigma, St Louis, MO) at 37^{o}C for 60 min. Immuno-staining of cells and counter staining with propidium iodide (PI) for high throughput quantitative analysis by Acumen Explorer were similarly done as described (3).

UV irradiation and FACS analysis

UV irradiation was performed at 254 nm (UV-C) using a Stratalinker 2400 (Stratagene) on U2OS cells under the same conditions as described by Manke et al (36). U2OS cells were prepared for FACS analysis also as described by Manke et al (36).

In addition to experiments reproducing the Manke et al. UV damage data, additional UV experiments were performed at 290nm (UV-B) using a Bio-Link BLX (Vilber Lourmat) computerized UV cross linker. For all UV-B experiments, cells were treated with UV-B, as indicated in the figure legends, after removal of cell growth media, followed immediately by re-introduction of growth media with indicated chemical inhibitor treatments. Western Blot, FACS and Acumen high content imaging experiments were performed as previously described (3, 11, 47).

Gene expression profiling analysis

Microarray analysis was performed as previously described (30). Briefly, total RNA from Calu6 cells was isolated with RNA STAT-60 (Tel-Test) according to the manufacturer's protocol. 5 micrograms of total RNA were labeled and hybridized to Affymetrix U133plus2 arrays according to the Affymetrix protocol. All samples were assessed for RNA quality such as microarray scaling factors, background levels, percent present calls, ß-actin and GAPDH 3'/5' ratios, etc. Signal intensities as gene expression values were obtained from Microarray Suite version 5.0 (MAS5) using the default settings, except 2% trimmed mean was set to 1500. To apply statistical analysis, a two-sided t-test was used to identify genes differentially expressed between two groups. The p values of the t-tests were adjusted for multiple testing using the false discovery rate. The adjusted P values, or the false discovery rates (FDR), are designated as Q values, where Q = P*n/I (n = total

number of probe sets on the microarrays; i = sorted rank of P values). The fold change was calculated as the ratio of the two group means based on the observed signal values from MAS5 and the gene expression signal change was calculated as the difference of the two group means. The criteria to define differential gene expression are FDR < 0.05, fold change > 1.4 and absolute change > 250. Differentially expressed genes were mapped to Gene Ontology (GO) biological process categories and KEGG pathways. The significance of GO terms or KEGG pathways over-represented in differentially expressed genes was tested using the hyper-geometric distribution function adjusted with family-wise error rates for multiple pairwise tests.

Figure Legends

Figure 1: DNA damage induces G_2 arrest and activates p38 MAPK and Chk1 pathways. (A) Cell-cycle profiles of control HeLa cells or HeLa cells treated with 160nM adriamycin or 500J/M^2 UV irradiation or 0.01% MMS for 24 hours; (B,C) Western blot analysis of activation of p38α and phosphorylation of its substrate MAPKAPK-2 (MK2) in unsynchronized HeLa cells treated with increasing doses of UV irradiation with 10μg/ml anisomycin treatment as a positive control (B); with 0.01% MMS for various time intervals for up to 10 hours (C); (D) synchronized HeLa cells treated with 160nM adriamycin 5 hours after release from second thymidine block. Cell cycle progression and p38 activation were analyzed by flow cytometry and Western blot at time points indicated after release; (E-G) DNA Damage in synchronized cells: HeLa cells synchronized at G1 by serum starvation (E), at G_1/S by double thymidine block (F) and at G_2 with CDK1 inhibitor RO-3306 (G) and then were released into 0.01% MMS-containing fresh medium. Activation of p38 and Chk1 kinases were followed by Western blot at time intervals indicated.

Figure 2: Inhibition of Chk1 but not p38 abrogates G_2 DNA damage checkpoint in HeLa cells. (A) Mitotic index of unsynchronized HeLa cells that were pre-treated for 20 hours with adriamycin prior to the addition of 320nM p38 inhibitor (p38i), or 1.25μMChk1 inhibitor (Chk1i) and 150nM nocodazole. Mitotic index were quantified using the high content/high throughput Acumen Explorer for cells expressing phospho-histone H3 at time points indicated after inhibitor treatment; (B) Western blot analysis of double thymidine synchronized HeLa cells treated with various kinase inhibitors in the presence

of 160nM adriamycin and 150 nM nocodazole 20 hours after release from thymidine block. Lane 1: double thymidine treated cells; lane 2: untreated HeLa cells; Lanes 3-9: synchronized cells treated with adriamycin; lane 3: adriamycin alone; lane 4: plus 320nM p38 inhibitor (p38i); lane 5: plus 2μM MK2 inhibitor (MK2i); lane 6: plus 1.25μM Chk1 inhibitor (Chk1i): lane 7: plus 6mM caffeine; lane 8: plus 1.25μM Chk1i+320nM p38i; lane 9: plus 6mM caffeine +320nM p38i; (C) Western blot analysis of the relationship between p38 activation/inactivation and DNA damage response. Thymidine synchronized HeLa cells were released into 0.01% MMS and cells were analyzed at times indicated; (D) Mitotic index of unsynchronized Hela cells treated with 500J/M^2 UV-B irradiation for 20 hours prior to addition of 320nM p38 inhibitor (p38i) or 1.25μM Chk1 inhibitor (Chk1i) in the presence of 150nM nocodazole (Noc); (E) Western Blot of HeLa cells treated with 1000J/M^2 UV-B and indicated doses of p38 inhibitor (p38i), MK2 inhibitor (MK2i) or Chk1 inhibitor (Chk1i) 24 hours after kinase inhibitor treatment.

Figure 3: Inhibition of Chk1 but not p38 by small molecule kinase inhibitors or RNAi abrogates UV induced G_2 DNA damage checkpoint. (A) Western blot analysis of response of cells after inactivation of Chk1, p38 or MK2 by 2 specific and validated siRNA oligonucleotides directed against each gene to adriamycin; (B) Mitotic Index plot of HeLa cells with p38 or Chk1 knockdown and treated with 160nM adriamycin or 500J/M^2 UV for 24 hours; (C) p53-dependent abrogation of G_2 DNA damage checkpoint by Chk1 inhibition. A549, U2OS and Calu-6 cancer cells were treated with 160 nM adriamycin for 24 hours before addition of kinase inhibitors (320nM p38i or 1.25μM Chk1i). Mitotic index were determined at 3 and 24 hours after addition of kinase inhibitors; (D-E) MK2 is not required for G2 DNA damage checkpoint control following

UV-C irradiation. U2OS cells treated with GFP or MK2 (MAPKAP kinase-2) siRNA were irradiated with 20J/M^2 of UV-C as described previously (32), and then placed in 50ng/ml nocodazole-containing medium for additional 16 hours. Target protein knockdown, DNA content and phospho-histone H3 of cells were analyzed by Western blotting (D) and flow cytometry (E).

Figure 4: Non-genotoxic activation of p38 with anisomycin does not impede entry into mitosis in HeLa cells. (A) Mitotic Index (phospho-histone H3) of HeLa cells synchronized with CDK1 inhibitor RO-3306 in the presence or absence of 2μg/ml anisomycin; (B) Western Blot for p38 activation of HeLa cells synchronized with CDK1 inhibitor RO3306 by 2μg/ml anisomycin.

Figure 5: Inactivation of p38 inhibits immediate early response and anti-apoptotic pathways in TNF-α treated Calu-6 cells. (A) Cluster analysis of genes differentially expressed 1 hour after TNF-α treatment and effect of 320nM p38i LY479754, on these expression changes. Gene expression values are represented by colors with red and green color indicate high and low expressions, respectively; (B) Box-plots of TNFα response of immediate early response genes and members of apoptosis pathway component genes at 1 hour time point in the presence or absence of p38 kinase inhibitor. (C) Western Blots of p38 activation, apoptosis and cell death/survival pathway protein expression in Calu-6 cells treated with TNF-α in the presence of 320nM p38i, LY479754. (D) Apoptotic index (% of cells expressing cleaved-PARP) of Calu-6 cells treated with 25ng/ml TNF-α and various concentrations of p38i using an Acumen Explorer high content imaging assay. CTRL = control with no treatment.

Figure 6: Inhibition of p38 MAPK sensitizes cells to adriamycin and induces cell death. (A) Apoptosis Index (% of cells expressing cleaved-caspase 3) of HeLa cells treated with increasing doses of p38i, LY479754, in the presence of 160nM adriamycin for 48 hours; (B) Western blot for apoptosis of HeLa cells treated with siRNA targeting p38α, MK2 or Chk1 in the presence or absence of 160nM adriamycin for 48 hours; (C) Western Blot analysis of synchronized A549 cells by serum starvation for 48 hours after treatment with 1μM p38i, LY479754, in the presence of DNA damage induced by 160nM adriamycin for 48 hours; (D) Western Blot of A549 cells treated with 0.01% MMS and 1μM p38i, LY479754, for 48 hours; (E) apoptosis induced by p38 inhibition in the presence of DNA damage is associated with G2 arrest. Apoptosis Index and cell cycle state were determined in A549 cells treated with 160nM adriamycin and 1μM p38i, LY479754, using the Acumen Explorer.

Figure 7: A new Model for a novel role of p38 MAPK in DNA damage response in cancer cells. DNA damage elicits the activation of cell cycle checkpoint, DNA repair and cell survival signaling pathways. In response to DNA damage, Chk1-mediated G_2 DNA damage checkpoint is activated to prevent entry into mitosis with damaged DNA, whereas p38-mediated cell survival pathway is activated to keep cells alive. Together, these two pathways afford cell the time to repair DNA damage and ultimately to allow recovery from DNA damage.

Acknowledgements

The authors would like to thank Li Fan of Ye's lab and Chris Sim Kim Siew, Connie Er Poh Nee at Systems Biology, Lilly Singapore Center for Drug Discovery Pte Ltd. for their technical assistance. We would like to thank Dr. Song Qing Na and Dr. Mark Marshall for providing the MAPKAPK2 (MK2) inhibitor and the Chk1 inhibitor, respectively. We would like to acknowledge Xi Lin for her assistance in running the microarrays and Dr. Shuguang Huang for initial gene expression profiling analysis. We would also like to thank Dr. Gunaretnam (Guna) Rajagopal (NJ Cancer Institute) for his help in this work.

690

691 Reference List

692

693 1. **Bain, J., L. Plater, M. Elliott, N. Shpiro, C. J. Hastie, H. McLauchlan, I.**
694 **Klevernic, J. S. Arthur, D. R. Alessi, and P. Cohen**. 2007. The selectivity of
695 protein kinase inhibitors: a further update. Biochem. J. **408**:297-315.

696 2. **Blasina, A., J. Hallin, E. Chen, M. E. Arango, E. Kraynov, J. Register, S.**
697 **Grant, S. Ninkovic, P. Chen, T. Nichols, P. O'Connor, and K. Anderes**. 2008.
698 Breaching the DNA damage checkpoint via PF-00477736, a novel small-molecule
699 inhibitor of checkpoint kinase 1. Mol. Cancer Ther. **7**:2394-2404.

700 3. **Bowen, W. P. and P. G. Wylie**. 2006. Application of laser-scanning fluorescence
701 microplate cytometry in high content screening. Assay. Drug Dev. Technol.
702 **4**:209-221.

703 4. **Bucher, N. and C. D. Britten**. 2008. G2 checkpoint abrogation and checkpoint
704 kinase-1 targeting in the treatment of cancer. Br. J Cancer. **98**:523-528.

705 5. **Bulavin, D. V., Y. Higashimoto, I. J. Popoff, W. A. Gaarde, V. Basrur, O.**
706 **Potapova, E. Appella, and A. J. Fornace, Jr.** 2001. Initiation of a G2/M
707 checkpoint after ultraviolet radiation requires p38 kinase. Nature. **411**:102-107.

708 6. **Bulavin, D. V., S. Saito, M. C. Hollander, K. Sakaguchi, C. W. Anderson, E.**
709 **Appella, and A. J. Fornace, Jr.** 1999. Phosphorylation of human p53 by p38

kinase coordinates N-terminal phosphorylation and apoptosis in response to UV radiation. EMBO J. **18**:6845-6854.

7. **de, D. A., C. Shih, U. B. Lopez de, C. Sanchez, P. M. del, L. M. Martin Cabrejas, S. Pleite, J. Blanco-Urgoiti, M. J. Lorite, C. R. Nevill, Jr., R. Bonjouklian, J. York, M. Vieth, Y. Wang, N. Magnus, R. M. Campbell, B. D. Anderson, D. J. McCann, D. D. Giera, P. A. Lee, R. M. Schultz, L. C. Li, L. M. Johnson, and J. A. Wolos**. 2005. Design of potent and selective 2-aminobenzimidazole-based p38alpha MAP kinase inhibitors with excellent in vivo efficacy. J Med. Chem. **48**:2270-2273.

8. **Didier, C., C. Cavelier, M. Quaranta, M. O. Galcera, C. Demur, G. Laurent, S. Manenti, and B. Ducommun**. 2008. G2/M checkpoint stringency is a key parameter in the sensitivity of AML cells to genotoxic stress. Oncogene. **%19;27**:3811-3820.

9. **Enders, G. H.** 2008. Expanded roles for Chk1 in genome maintenance. J Biol. Chem. **283**:17749-17752.

10. **Fabian, M. A., W. H. Biggs, III, D. K. Treiber, C. E. Atteridge, M. D. Azimioara, M. G. Benedetti, T. A. Carter, P. Ciceri, P. T. Edeen, M. Floyd, J. M. Ford, M. Galvin, J. L. Gerlach, R. M. Grotzfeld, S. Herrgard, D. E. Insko, M. A. Insko, A. G. Lai, J. M. Lelias, S. A. Mehta, Z. V. Milanov, A. M. Velasco, L. M. Wodicka, H. K. Patel, P. P. Zarrinkar, and D. J. Lockhart**.

2005. A small molecule-kinase interaction map for clinical kinase inhibitors. Nat. Biotechnol. **23**:329-336.

11. **Fan, L., X. Yang, J. Du, M. Marshall, K. Blanchard, and X. Ye**. 2005. A novel role of p38 alpha MAPK in mitotic progression independent of its kinase activity. Cell Cycle. **4**:1616-1624.

12. **Flacke, J. P., S. Kumar, S. Kostin, H. P. Reusch, and Y. Ladilov**. 2009. Acidic preconditioning protects endothelial cells against apoptosis through p38- and Akt-dependent Bcl-xL overexpression. Apoptosis. **14**:90-96.

13. **Gatti, G., G. Maresca, M. Natoli, F. Florenzano, A. Nicolin, A. Felsani, and I. D'Agnano**. 2009. MYC prevents apoptosis and enhances endoreduplication induced by paclitaxel. PLoS. ONE. **4**:e5442.

14. **Grethe, S., M. P. Ares, T. Andersson, and M. I. Porn-Ares**. 2004. p38 MAPK mediates TNF-induced apoptosis in endothelial cells via phosphorylation and downregulation of Bcl-x(L). Exp. Cell Res. **298**:632-642.

15. **Guan, Z., S. Y. Buckman, A. P. Pentland, D. J. Templeton, and A. R. Morrison**. 1998. Induction of cyclooxygenase-2 by the activated MEKK1 --> SEK1/MKK4 --> p38 mitogen-activated protein kinase pathway. J Biol. Chem. **273**:12901-12908.

16. **Hamanoue, M., K. Sato, and K. Takamatsu**. 2007. Inhibition of p38 mitogen-activated protein kinase-induced apoptosis in cultured mature oligodendrocytes using SB202190 and SB203580. Neurochem. Int. **51**:16-24.

17. **Han, J., J. D. Lee, L. Bibbs, and R. J. Ulevitch**. 1994. A MAP kinase targeted by endotoxin and hyperosmolarity in mammalian cells. Science. **265**:808-811.

18. **Han, J., J. D. Lee, P. S. Tobias, and R. J. Ulevitch**. 1993. Endotoxin induces rapid protein tyrosine phosphorylation in 70Z/3 cells expressing CD14. J Biol. Chem. **268**:25009-25014.

19. **Hirose, Y., M. Katayama, M. S. Berger, and R. O. Pieper**. 2004. Cooperative function of Chk1 and p38 pathways in activating G2 arrest following exposure to temozolomide. J. Neurosurg. **100**:1060-1065.

20. **Hynes, J., Jr. and K. Leftheri**. 2005. Small molecule p38 inhibitors: novel structural features and advances from 2002-2005. Curr. Top. Med. Chem. **5**:967-985.

21. **Jackson, J. R., A. Gilmartin, C. Imburgia, J. D. Winkler, L. A. Marshall, and A. Roshak**. 2000. An indolocarbazole inhibitor of human checkpoint kinase (Chk1) abrogates cell cycle arrest caused by DNA damage. Cancer Res. **60**:566-572.

22. **Jurvansuu, J., M. Fragkos, C. Ingemarsdotter, and P. Beard**. 2007. Chk1 instability is coupled to mitotic cell death of p53-deficient cells in response to virus-induced DNA damage signaling. J Mol. Biol. **372**:397-406.

23. **Kim, M. J., S. Y. Choi, I. C. Park, S. G. Hwang, C. Kim, Y. H. Choi, H. Kim, K. H. Lee, and S. J. Lee**. 2008. Opposing roles of c-Jun NH2-terminal kinase and p38 mitogen-activated protein kinase in the cellular response to ionizing radiation in human cervical cancer cells. Mol. Cancer Res. **6**:1718-1731.

24. **Koniaras, K., A. R. Cuddihy, H. Christopoulos, A. Hogg, and M. J. O'Connell**. 2001. Inhibition of Chk1-dependent G2 DNA damage checkpoint radiosensitizes p53 mutant human cells. Oncogene. **20**:7453-7463.

25. **Kramer, A., N. Mailand, C. Lukas, R. G. Syljuasen, C. J. Wilkinson, E. A. Nigg, J. Bartek, and J. Lukas**. 2004. Centrosome-associated Chk1 prevents premature activation of cyclin-B-Cdk1 kinase. Nat. Cell Biol. **6**:884-891.

26. **Kurosu, T., Y. Takahashi, T. Fukuda, T. Koyama, T. Miki, and O. Miura**. 2005. p38 MAP kinase plays a role in G2 checkpoint activation and inhibits apoptosis of human B cell lymphoma cells treated with etoposide. Apoptosis. **10**:1111-1120.

27. **Kyriakis, J. M. and J. Avruch**. 1996. Sounding the alarm: protein kinase cascades activated by stress and inflammation. J Biol. Chem. **271**:24313-24316.

28. **Kyriakis, J. M. and J. Avruch**. 1996. Sounding the alarm: protein kinase cascades activated by stress and inflammation. J Biol. Chem. **271**:24313-24316.

29. **Levesque, A. A., A. A. Fanous, A. Poh, and A. Eastman**. 2008. Defective p53 signaling in p53 wild-type tumors attenuates p21waf1 induction and cyclin B repression rendering them sensitive to Chk1 inhibitors that abrogate DNA damage-induced S and G2 arrest. Mol. Cancer Ther. **7**:252-262.

30. **Li, S., H. Y. Zhang, C. C. Hu, F. Lawrence, K. E. Gallagher, A. Surapaneni, S. T. Estrem, J. N. Calley, G. Varga, E. R. Dow, and Y. Chen**. 2008. Assessment of diet-induced obese rats as an obesity model by comparative functional genomics. Obesity. (Silver. Spring). **16**:811-818.

31. **Lim, S. J., Y. J. Lee, and E. Lee**. 2006. p38MAPK inhibitor SB203580 sensitizes human SNU-C4 colon cancer cells to exisulind-induced apoptosis. Oncol. Rep. **16**:1131-1135.

32. **Manke, I. A., A. Nguyen, D. Lim, M. Q. Stewart, A. E. Elia, and M. B. Yaffe**. 2005. MAPKAP kinase-2 is a cell cycle checkpoint kinase that regulates the G2/M transition and S phase progression in response to UV irradiation. Mol. Cell. **17**:37-48.

33. **Mikhailov, A., D. Patel, D. J. McCance, and C. L. Rieder**. 2007. The G2 p38-mediated stress-activated checkpoint pathway becomes attenuated in transformed cells. Curr. Biol. **17**:2162-2168.

34. **Moriguchi, T., H. Kawasaki, S. Matsuda, Y. Gotoh, and E. Nishida**. 1995. Evidence for multiple activators for stress-activated protein kinase/c-Jun amino-terminal kinases. Existence of novel activators. J Biol. Chem. **270**:12969-12972.

35. **Ono, K. and J. Han**. 2000. The p38 signal transduction pathway: activation and function. Cell Signal. **12**:1-13.

36. **Pedraza-Alva, G., M. Koulnis, C. Charland, T. Thornton, J. L. Clements, M. S. Schlissel, and M. Rincon**. 2006. Activation of p38 MAP kinase by DNA double-strand breaks in V(D)J recombination induces a G2/M cell cycle checkpoint. EMBO J. **25**:763-773.

37. **Pietersma, A., B. C. Tilly, M. Gaestel, J. N. de, J. C. Lee, J. F. Koster, and W. Sluiter**. 1997. p38 mitogen activated protein kinase regulates endothelial VCAM-1 expression at the post-transcriptional level. Biochem. Biophys. Res. Commun. **230**:44-48.

38. **Reinhard Emily, Kolodziej Stephen, Anderson David, Stehle Nathan, Vernier William, Lee Len, and Hegde Shridhar**. July 2004. USA patent US2004/0127519.

39. **Reinhardt, H. C., A. S. Aslanian, J. A. Lees, and M. B. Yaffe**. 2007. p53-deficient cells rely on ATM- and ATR-mediated checkpoint signaling through the p38MAPK/MK2 pathway for survival after DNA damage. Cancer Cell. **11**:175-189.

40. **Rouse, J., P. Cohen, S. Trigon, M. Morange, A. onso-Llamazares, D. Zamanillo, T. Hunt, and A. R. Nebreda**. 1994. A novel kinase cascade triggered by stress and heat shock that stimulates MAPKAP kinase-2 and phosphorylation of the small heat shock proteins. Cell. **78**:1027-1037.

41. **Sakamoto, K. M. and D. A. Frank**. 2009. CREB in the pathophysiology of cancer: implications for targeting transcription factors for cancer therapy. Clin. Cancer Res. **15**:2583-2587.

42. **Schieven, G. L.** 2009. The p38alpha kinase plays a central role in inflammation. Curr. Top. Med. Chem. **9**:1038-1048.

43. **Vassilev, L. T.** 2006. Cell cycle synchronization at the G2/M phase border by reversible inhibition of CDK1. Cell Cycle. **5**:2555-2556.

44. **Wegiel, B., A. Bjartell, Z. Culig, and J. L. Persson**. 2008. Interleukin-6 activates PI3K/Akt pathway and regulates cyclin A1 to promote prostate cancer cell survival. Int. J Cancer. **122**:1521-1529.

45. **Xiao, Z., Z. Chen, A. H. Gunasekera, T. J. Sowin, S. H. Rosenberg, S. Fesik, and H. Zhang**. 2003. Chk1 mediates S and G2 arrests through Cdc25A degradation in response to DNA-damaging agents. J Biol. Chem. **278**:21767-21773.

46. **Xiao, Z., J. Xue, T. J. Sowin, and H. Zhang**. 2006. Differential roles of checkpoint kinase 1, checkpoint kinase 2, and mitogen-activated protein kinase-

activated protein kinase 2 in mediating DNA damage-induced cell cycle arrest: implications for cancer therapy. Mol. Cancer Ther. **5**:1935-1943.

47. **Yang, H., T. Burke, J. Dempsey, B. Diaz, E. Collins, J. Toth, R. Beckmann, and X. Ye**. 2005. Mitotic requirement for aurora A kinase is bypassed in the absence of aurora B kinase. FEBS Lett. **579**:3385-3391.

Figure 1

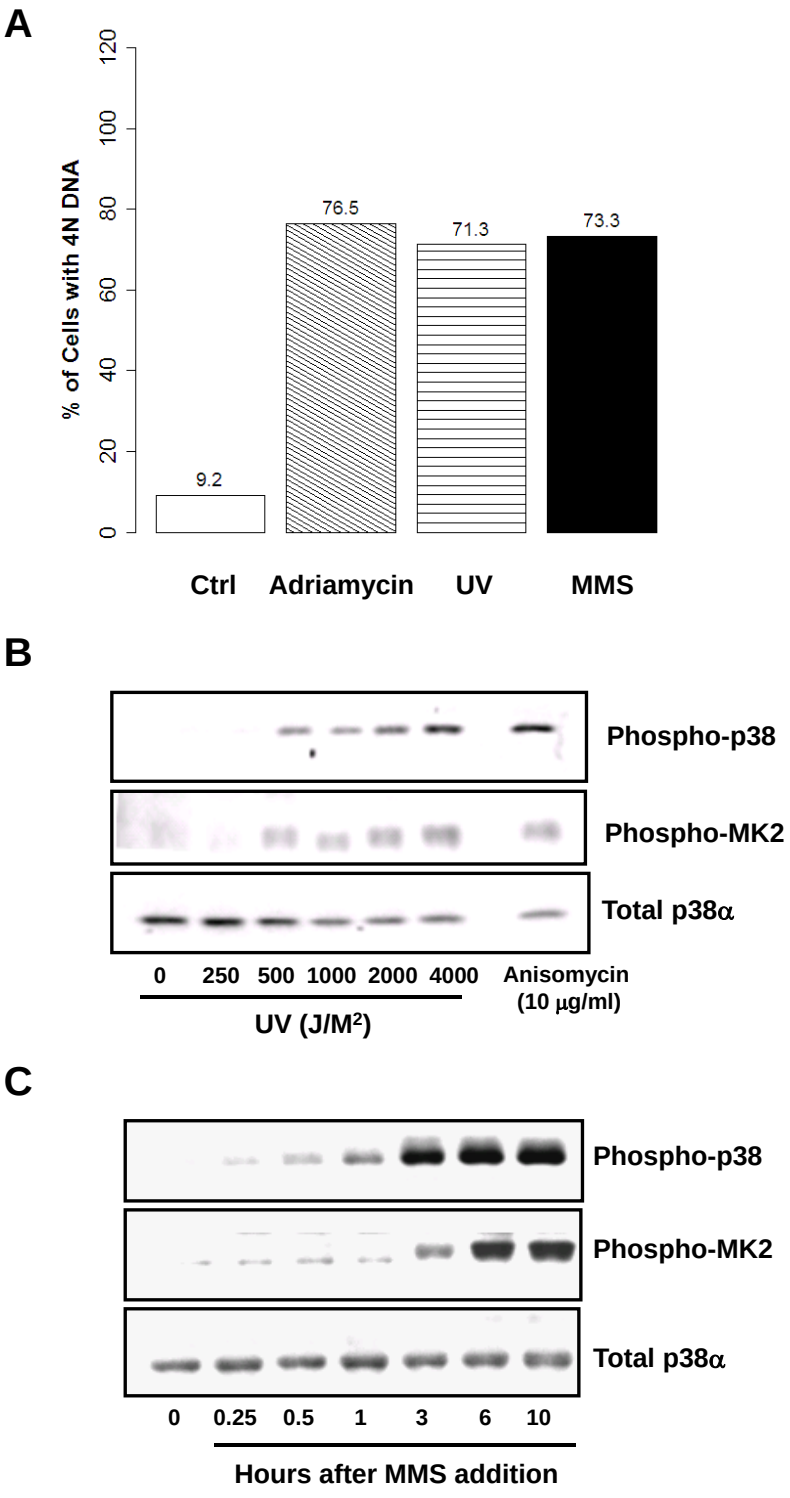

Figure 1, (Continued)

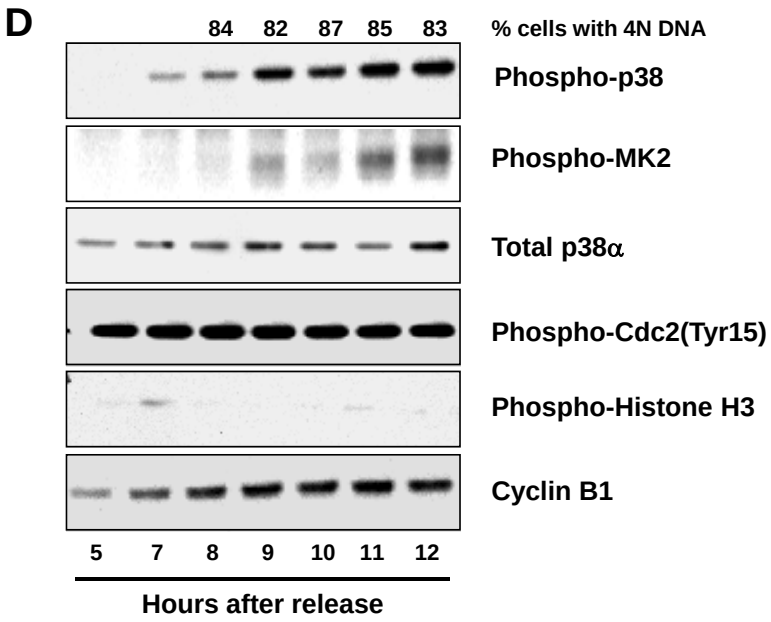

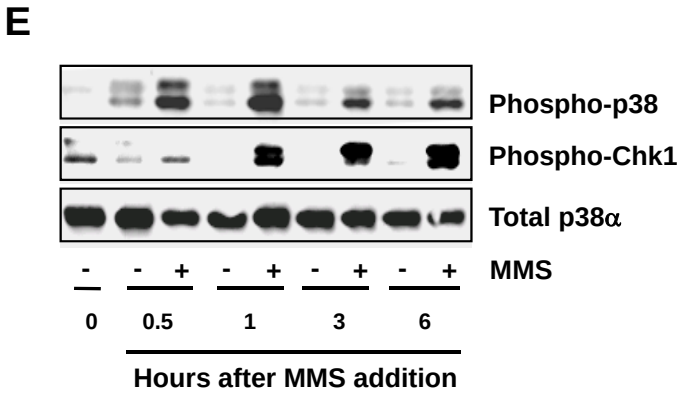

Figure 1, (Continued)

F

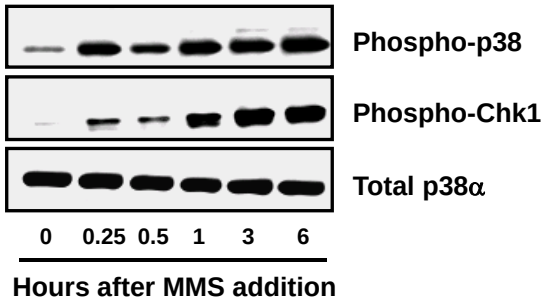

G

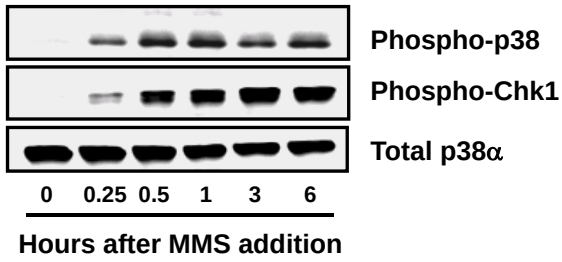

Figure 2

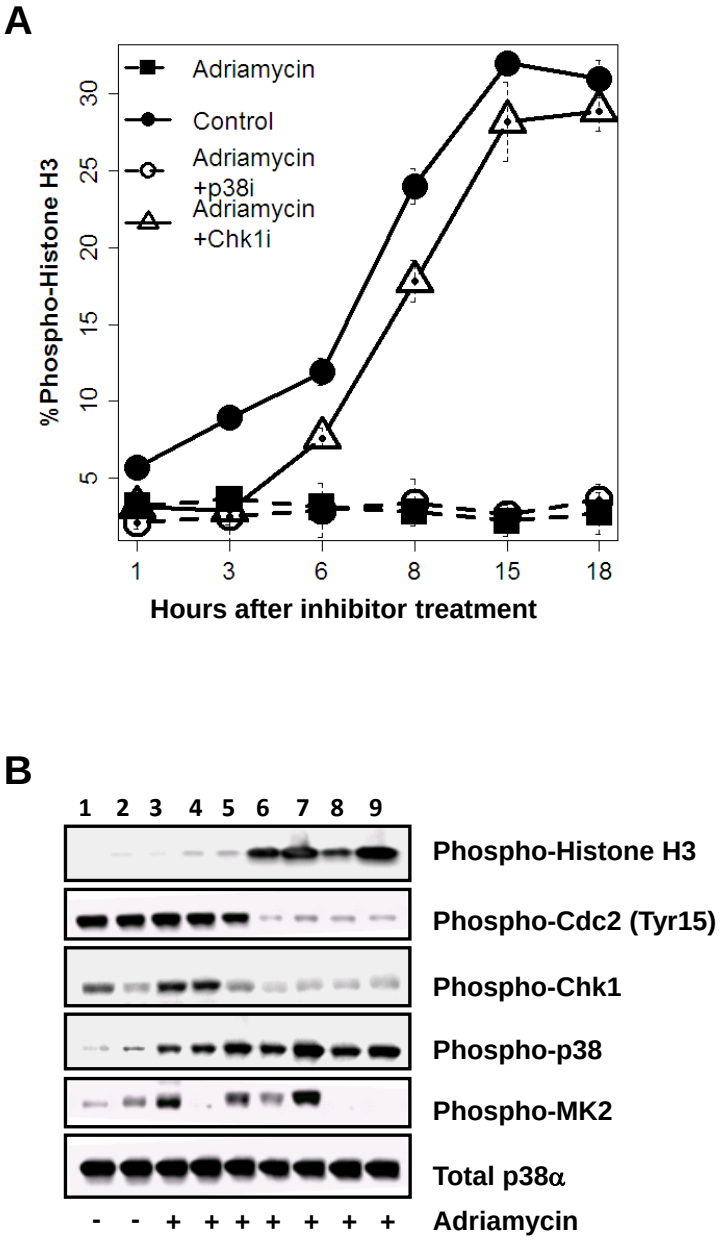

Figure 2, (continued)

C

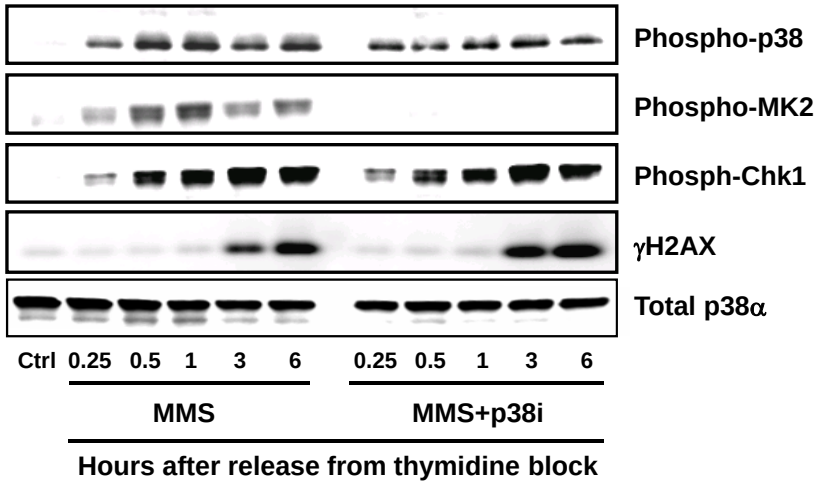

D

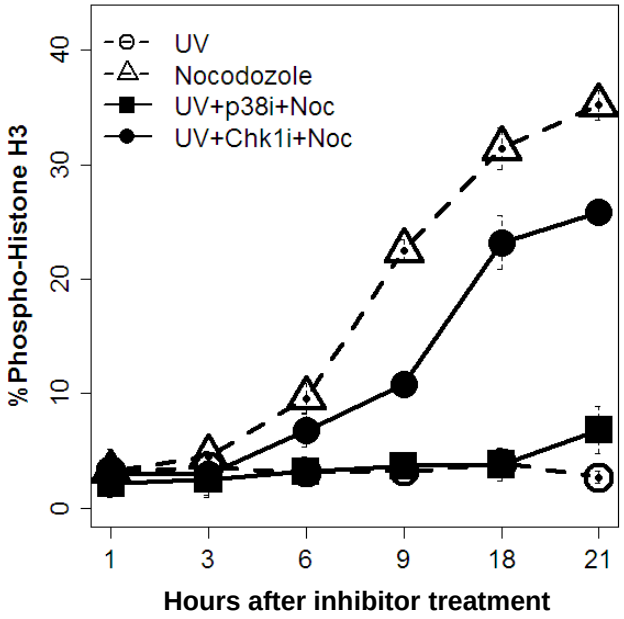

Figure 2, (continued)

E

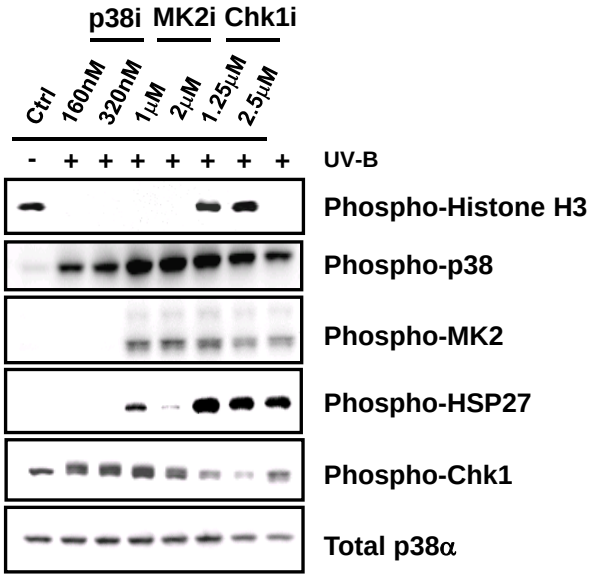

Figure 3

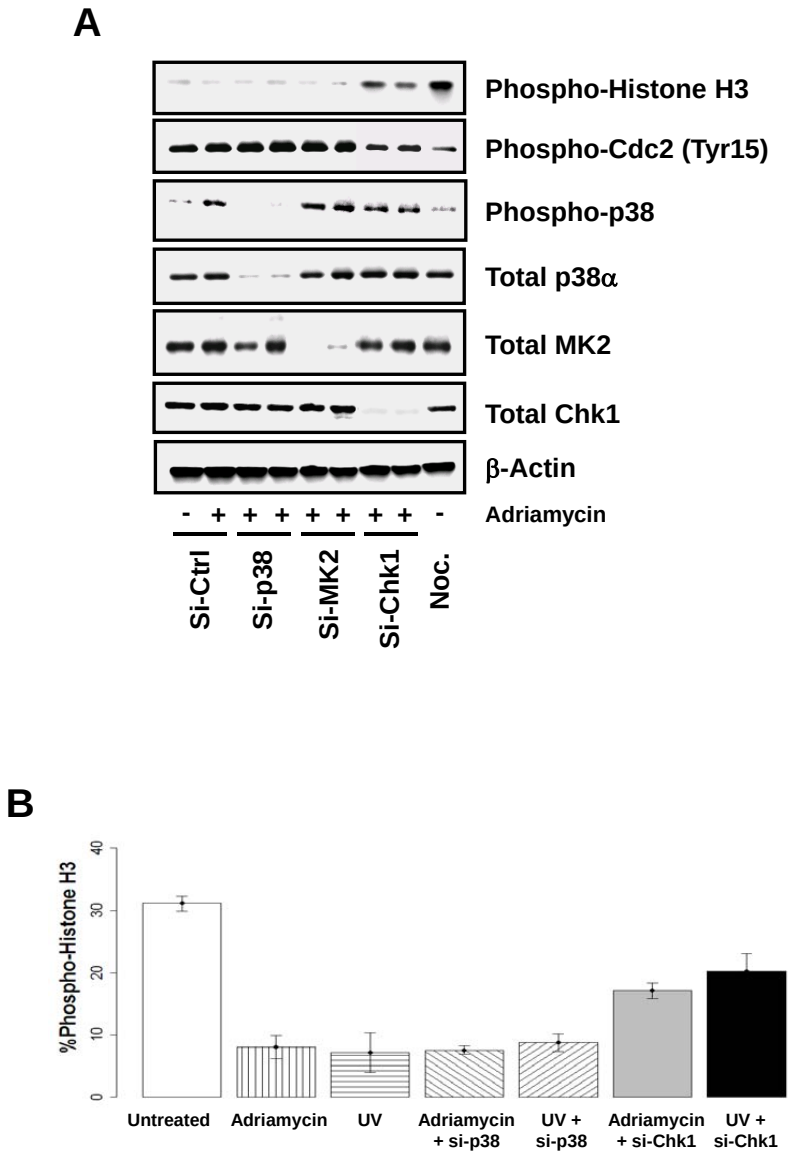

Figure 3, (continued)

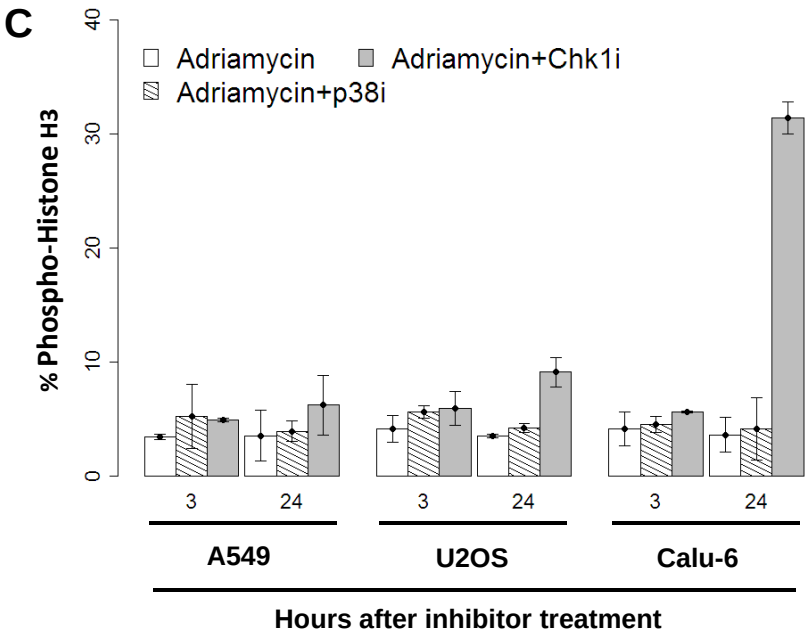

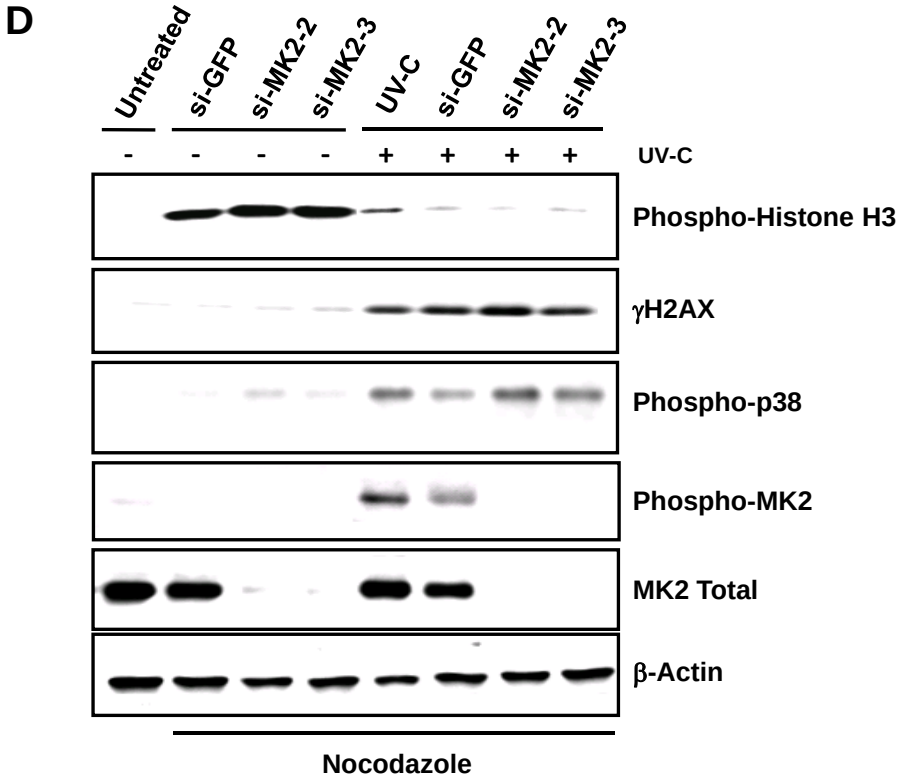

Figure 3, (continued)

E

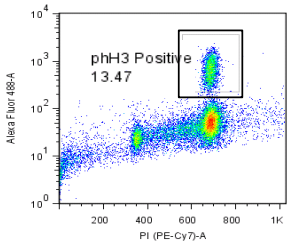

si-MK2

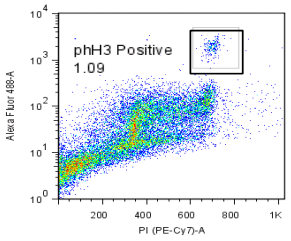

UV-C

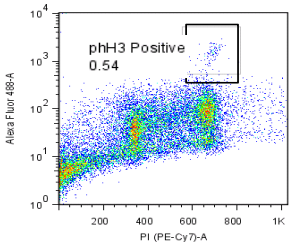

Si-MK2+ UV-C

Figure 4

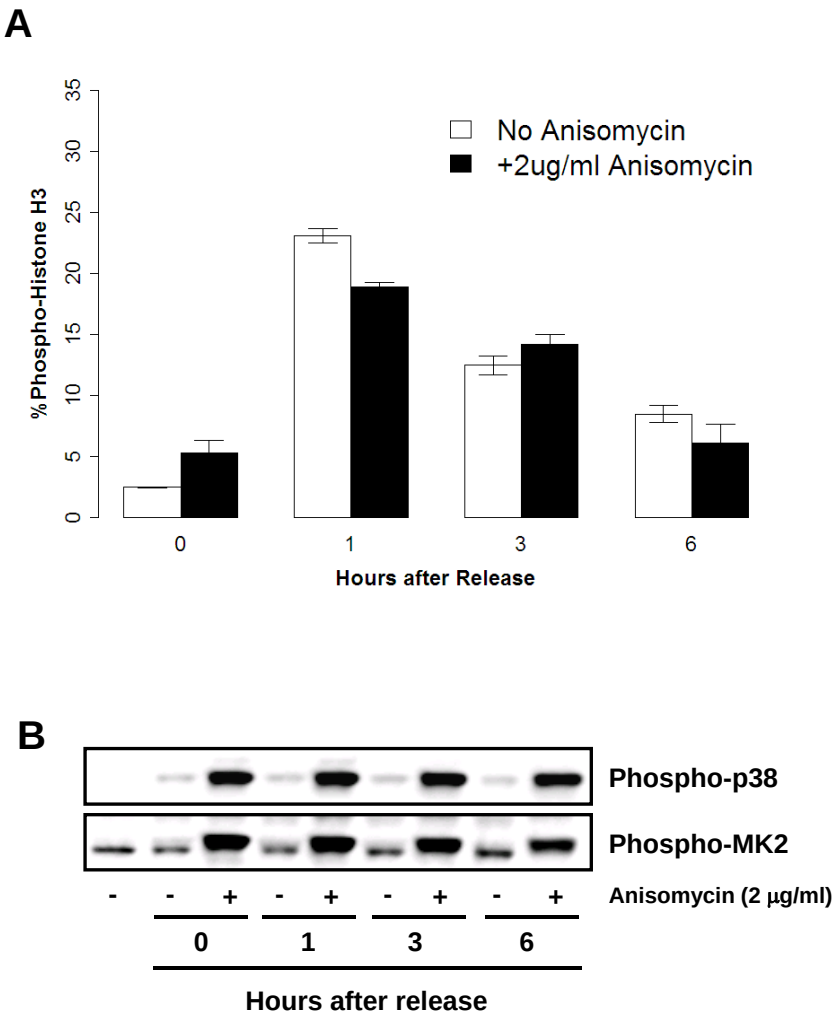

Figure 5

A

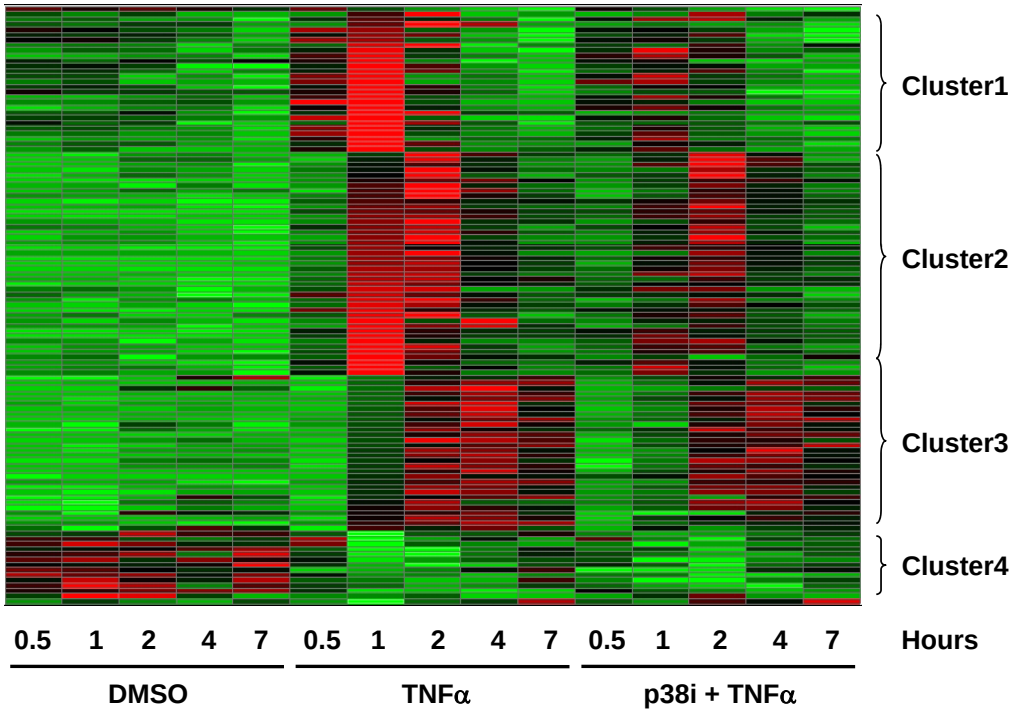

B

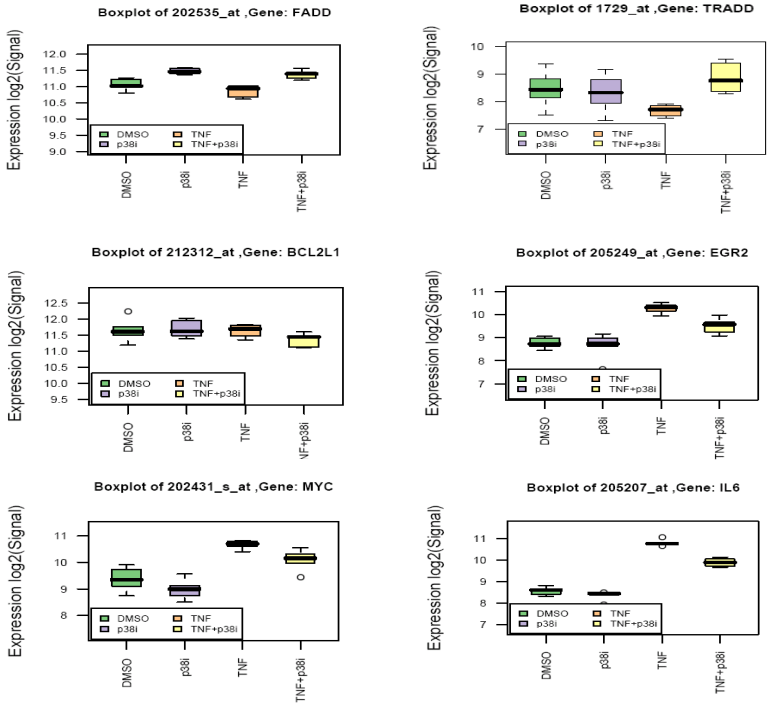

Figure 5, (continued)

C

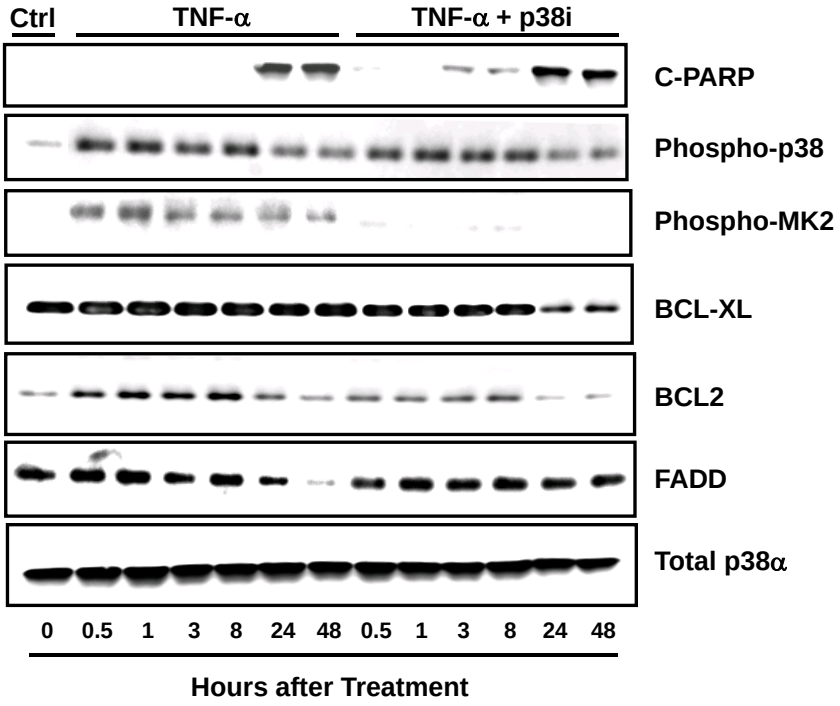

D

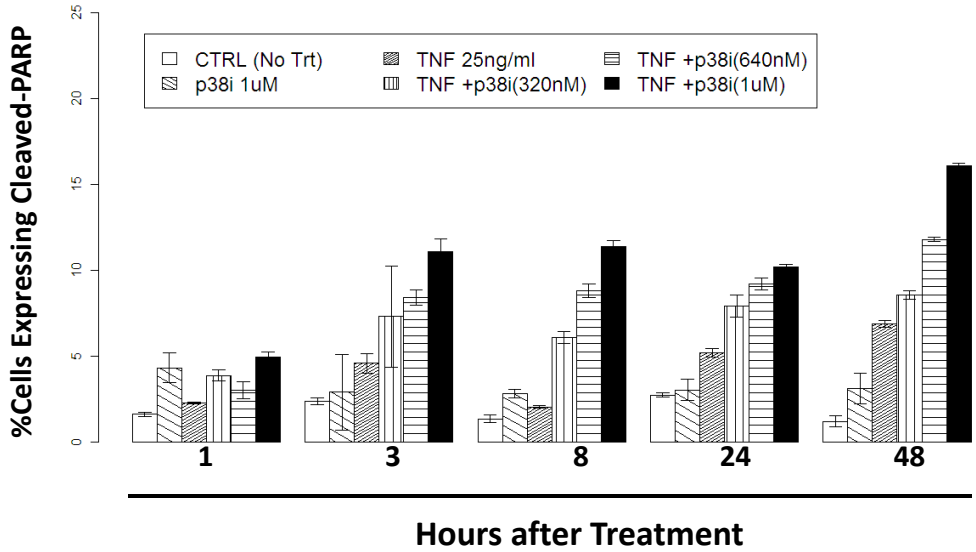

Figure 6

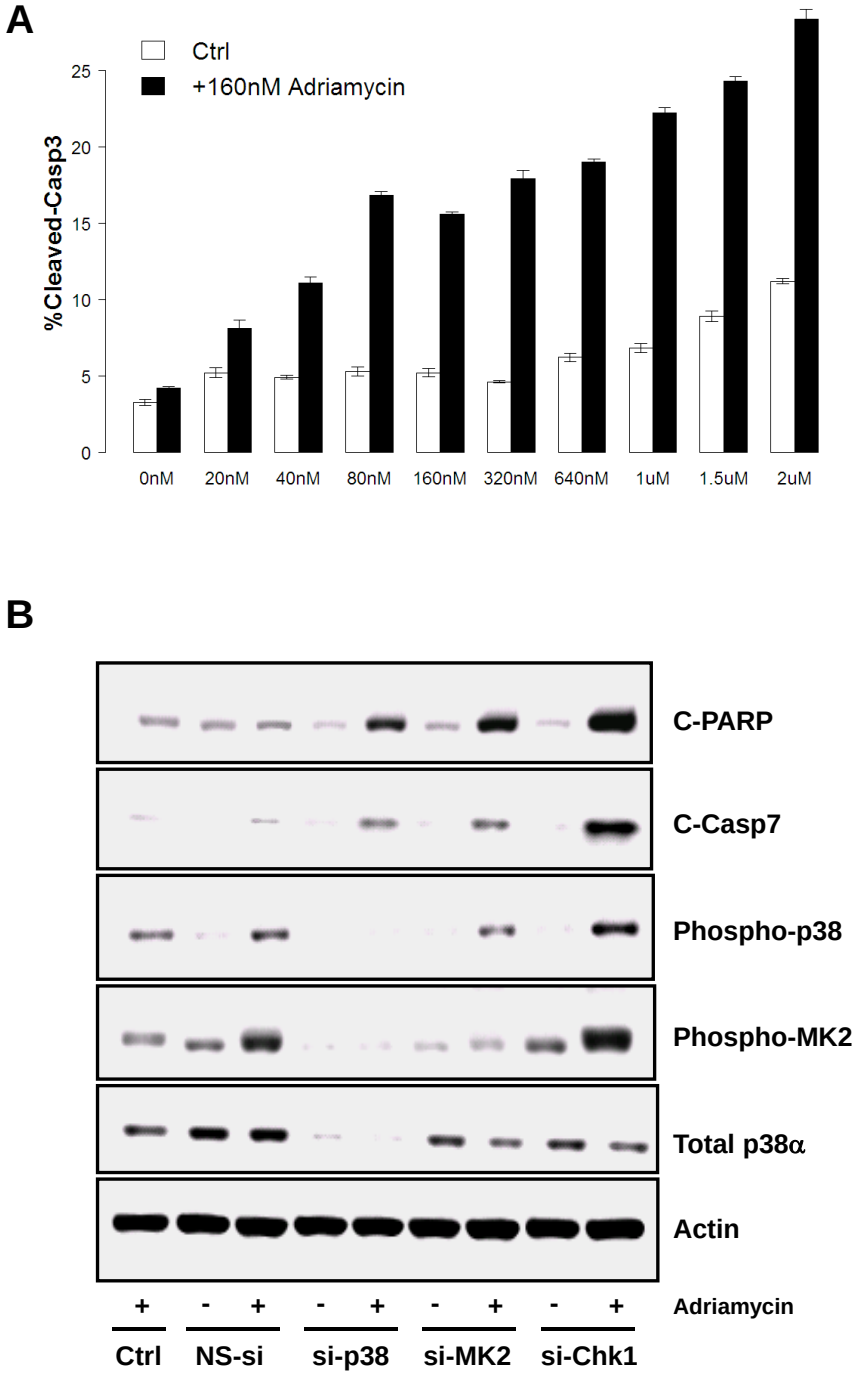

Figure 6, (continued)

C

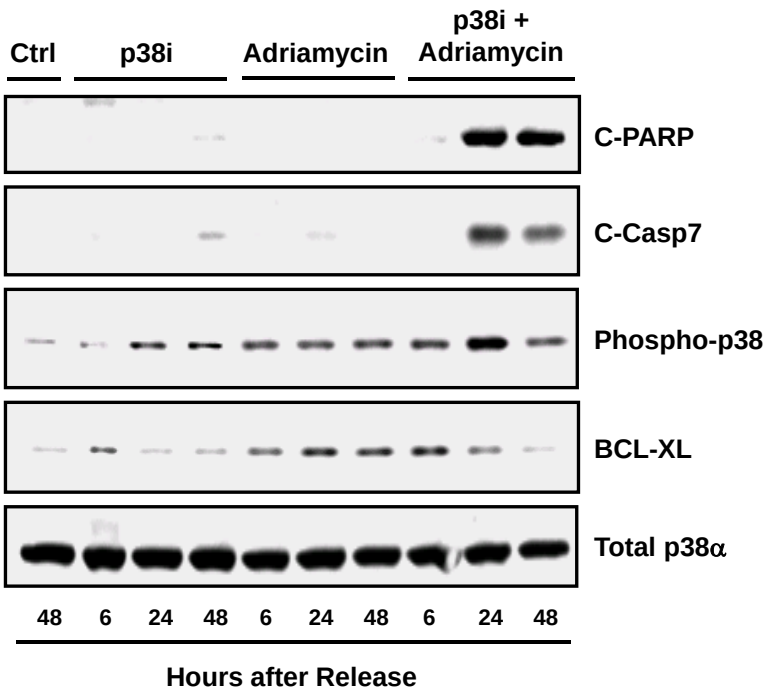

D

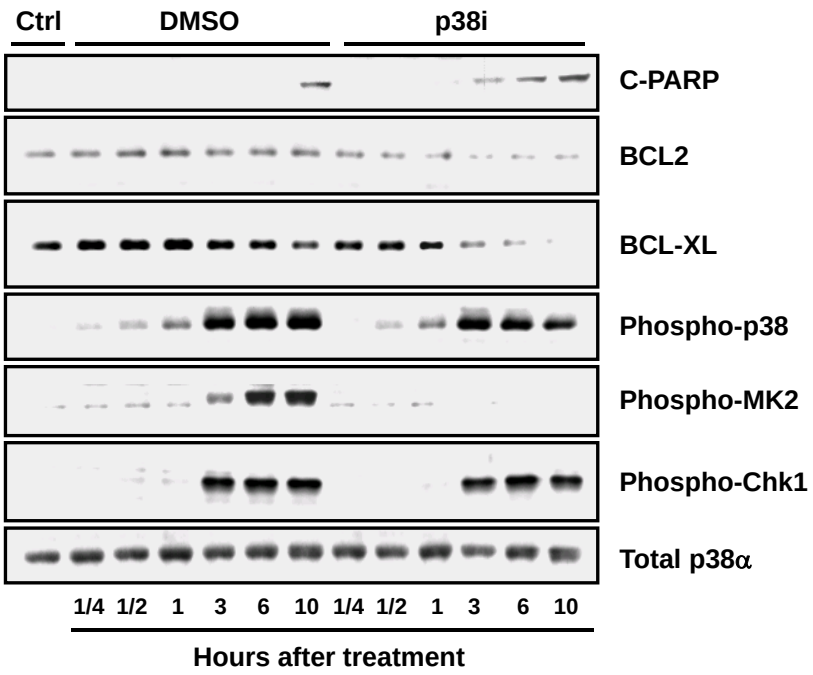

Figure 6, (continued)

E

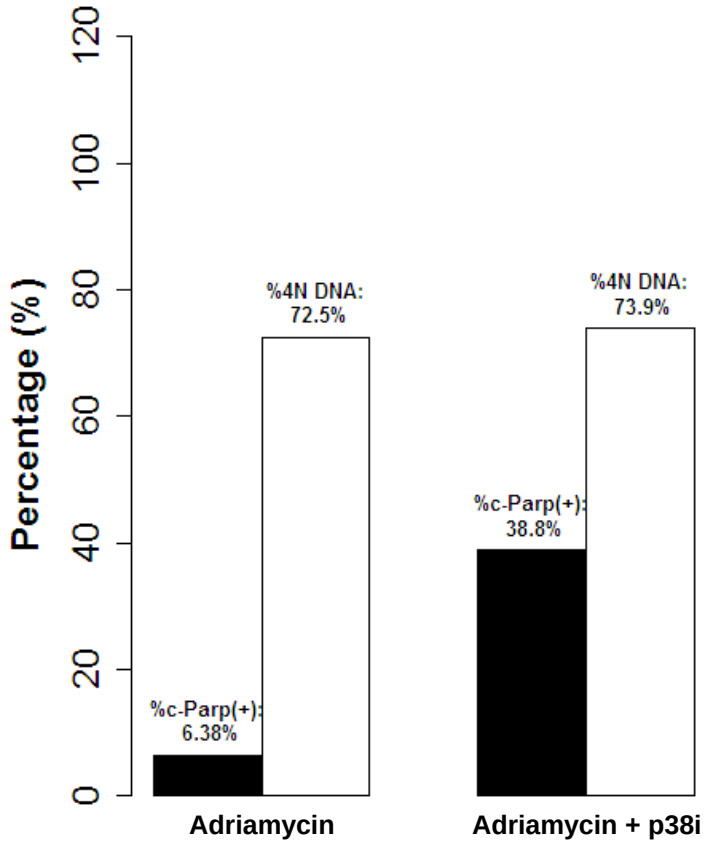

Figure 7